W-Band Filtering Antenna Based on a Slot Array and Stacked Coupled Resonators Using Gap Waveguide Technology

David Santiago, Mu Fang, Ashraf Uz Zaman, *Senior Member, IEEE*, Miguel A.G. Laso, *Fellow, IEEE*, Txema Lopetegi, *Member, IEEE*, and Ivan Arregui, *Member, IEEE*

***Abstract*—This letter proposes a new design approach for filtering antennas. The novel matching reflection coefficient-based method allows the integration of filters and antennas without compromising the frequency behavior of either of these components. Moreover, this integration is done by avoiding the need for lengthy optimization processes and provides a high degree of flexibility in the types of antennas that can be used. In order to validate it, two examples are provided. In both cases, a 4th-order Chebyshev bandpass filter at 101.5 GHz implemented in a stacked groove gap waveguide configuration is used, firstly along with a single aperture antenna and, subsequently, with a slotted ridge gap waveguide array. This second example has been manufactured to demonstrate the usefulness of the new design methodology. Excellent measured performance has been obtained for a filtering antenna at W-band for the first time.**

***Index Terms*—Bandpass filter, filtering antenna, gap waveguide, slot array antenna.**

I. Introduction

FILTERING antennas have gained significant attention in recent years due to their ability to integrate the functionalities of both an antenna and a filter in a single device, eliminating the need for any extra interface or transition. The main objective of a filtering antenna is to exhibit the aimed radiation characteristics within a specific passband while effectively suppressing undesired frequencies at designated stopbands. These components have found applications in diverse fields such as wireless communication, radar systems, satellite communication, and Internet-of-Things (IoT) devices, where simultaneous filtering and transmission/reception capabilities are essential.

Extensive research has been conducted on the integration of antennas and filters [1]. Different planar technologies have been employed for filtering antennas such as microstrip [2], [3], or the substrate-integrated waveguide (SIW) technology [4], [5], which are mainly suitable for low-frequency applications since their transmission properties greatly depend on the substrate parameters, suffering from high insertion loss at the millimeter-wave frequency range. Rectangular waveguide is well known as the technology that provides the lowest losses and has also been employed for this kind of device [6], [7], [8]. Nevertheless, ensuring electrical contact becomes very crucial when assembly and manufacturing needs to be done in a clamshell configuration, especially at high mmWave frequencies. Because of that, gap waveguide technology [9] emerged as an alternative at millimeter waves and has also been used in the design of filtering antenna devices, although not at frequencies higher than the Ka-band [10], [11], [12] and V-band [13].

Different design approaches for filtering antennas have been documented in the literature. The simplest strategy is to consider the antenna as a load element, as in [14], where a filter and an antenna, initially designed independently, are later interconnected using a coaxial line. An interesting approach is to embed the filter in the feeding network of the antenna, as done for instance in [11]. Another alternative is to integrate both components into one structure, sharing resonating cavities or other circuit elements. In order to do it, long optimization processes of the whole structure may be required, as in [8], where the S_{11}-parameter of the whole filtering antenna must be optimized to obtain the required dual-band response. Aiming to reduce the optimization time, other approaches based on the coupling matrix have been proposed in [6], [7]. In these works, a design parameter Q_r (radiation quality factor) is defined to model the filtering antenna and then, it is made to coincide with the external quality factor, $Q_{ext1,N}$, of the filter (where N is the number of resonators). Although this allows the integration of both the antenna and the filter, the frequency responses that can be achieved are constrained by the need to have a value of Q_r equal to $Q_{ext1,N}$ and its validity is limited to a reduced frequency range. Moreover, in order to have this equivalence, it is often necessary to modify the dimensions of the antenna, compromising its radiating behavior.

This letter presents a novel matching reflection coefficient-based method for the design of filtering antennas using gap waveguide technology, which allows the integration of the antenna and the filter in one device without compromising the radiating characteristics of the antenna and facilitates accomplishing wide band frequency devices if required. First, we will describe the technique employing a single radiating element and then we will validate its usefulness employing a more complex radiation structure such as a slotted ridge gap waveguide (RGW) array

Manuscript received 25 March 2024; accepted 4 May 2024. Date of publication 10 May 2024; date of current version 6 August 2024. This work was supported by the Spanish Ministerio de Ciencia e Innovación—Agencia Estatal de Investigación (MCIN/AEI/ 10.13039/501100011033) under Project PID2020-112545RB-C53 and funding for open access provided by Universidad Pública de Navarra. *(Corresponding author: David Santiago.)*

David Santiago, Miguel A.G. Laso, Txema Lopetegi, and Ivan Arregui are with the Institute of Smart Cities (ISC), Department of Electrical, Electronic, and Communications Engineering, Public University of Navarre (UPNA), 31006 Pamplona, Spain (e-mail: david.santiago@unavarra.es).

Mu Fang and Ashraf Uz Zaman are with the Department of Electrical Engineering, Chalmers University of Technology, 412 96 Gothenburg, Sweden.

Digital Object Identifier 10.1109/LAWP.2024.3399269

antenna. Excellent characteristics have been demonstrated for the first time for a filtering antenna at W-band in gap waveguide technology.

II. Design Method

The design procedure begins with the design of the filter as if it were an isolated structure. Therefore, a variety of filters implemented with different configurations can be considered. In this case, we will employ stacked resonator cavities coupled through an iris, as in [15], making the circuit footprint more compact. However, unlike [15], where RGW resonators are employed, higher-order-mode groove gap waveguide (GGW) resonators are used in our case. This allows the use of larger cavities that provide more robustness during fabrication using classical low-cost methods such as computer numerical control (CNC) milling, as explained in [16], where the TE_{103} mode was employed for this purpose using inline couplings. Additionally, higher-order modes in a stacked configuration allow us to modify the position of the iris, keeping the same coupling and, hence, having more flexibility and an extra variable to use during the design and further optimization, if needed, due to their field distribution along the cavity. In this step, we need to fix the filtering specifications determined by the order of the filter, *N*, the in-band return losses, *RL*, and the passband defined by its lower and upper frequencies, f_1 and f_2, respectively. For a bandpass between f_1 and f_2, the coupling between the resonating cavities, $K_{i,\ i+1}$, and the external quality factor, $Q_{ext1,N}$, are calculated as in [17]

$$K_{i,i+1} = \frac{BW}{\sqrt{g_i \cdot g_{i+1}}},\ i\ = 1, \ldots, N-1 \tag{1}$$

$$Q_{ext1,N} = \frac{g_0 \cdot g_1}{BW} \tag{2}$$

where *BW* is the fractional bandwidth and g_i are the equivalent low-pass filter coefficients. Once $K_{i,\ i+1}$ and $Q_{ext1,N}$ values are known, the dimensions and position of the irises ($w_{i,i+1}$, $t_{i,i+1}$, *Offset*) located in the bottom walls of the cavities can be determined as explained also in [17]. A cross-section of the stacked filter topology is shown in Fig. 1(a) along with a single cavity and an iris in Fig. 1(b).

Once the filter has been designed as an isolated structure, the second step involves focusing on its last stage, which we will refer to as the Filter Output Stage (FOS). Since the reflection coefficient of the FOS, denoted as Γ, is a key parameter in the design procedure, it is necessary to define the FOS precisely. The FOS in coupled cavity filters may consist of the filter output iris (responsible for the Q_{extN}), the last resonating cavity, and the last coupling iris (responsible for the coupling coefficient $k_{N\text{-}1,\ N}$) located on the bottom wall of the last cavity, as depicted in Fig. 1(c). The reflection coefficient of the FOS, Γ, is calculated over the bandwidth of interest using a full-wave electromagnetic simulator, such as CST MWS, and it will be the frequency response of an isolated resonator if it has been defined as previously explained. Actually, it would also be possible to evaluate Γ at any other position of the device, provided that the rest of the procedure is also performed consistently.

Once the FOS is evaluated, the third step of the method involves replacing the filter output of the FOS with the radiation element that will be used in the filtering antenna. The new structure, referred to as the Radiation Output Stage (ROS), is composed of the radiation element (for example, a single aperture), the last resonating cavity, and the last coupling iris,

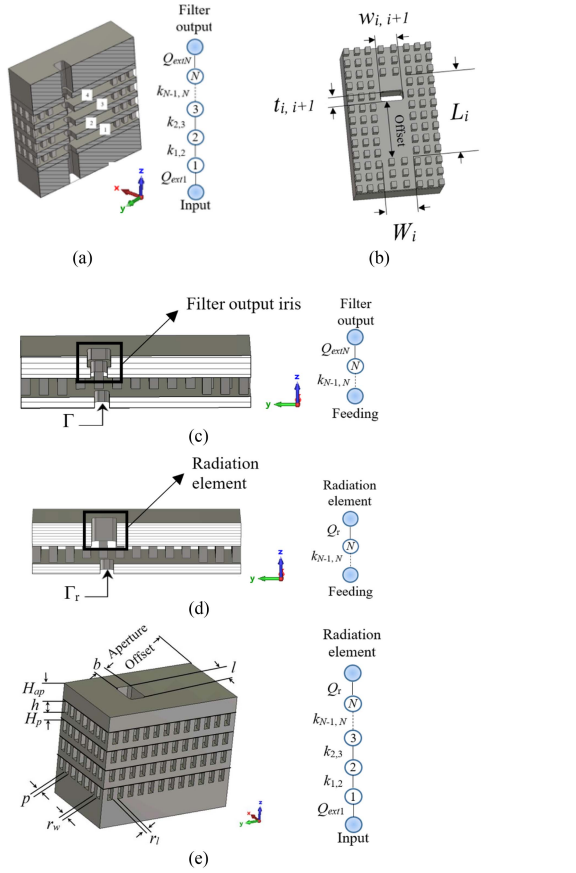

Fig. 1. Steps of the matching reflection coefficient-based method: (a) Schematic of a stacked BPF implemented in GGW; (b) schematic of a single cavity; (c) schematic of the filter output stage (FOS); (d) schematic of the radiation output stage (ROS); and (e) schematic of the stacked coupled-resonator filtering antenna using an aperture as a radiation element.

as illustrated in Fig. 1(d). The reflection coefficient of the ROS denoted as Γ_r, is calculated, and the aim in this step is to keep the reflection coefficient unaltered, ensuring that $\Gamma_r = \Gamma$ over the frequency of interest. This method is general for any kind of radiation element and valid as long as Γ_r replicates Γ, which would preserve the overall filtering characteristics. In order to achieve it, it is necessary to identify which variables of the ROS can be modified without altering the radiation characteristics, which must also remain unchanged. This will also depend on the radiating element used, as we will see in the examples below, and will ensure that the radiating characteristics of the antenna will not be modified when integrated with the filter.

After successfully replicating the reflection coefficient, the last step of the method consists of substituting the FOS of the filter previously designed with the final ROS since the rest of the filter remains unchanged in the filtering antenna. No further optimization is necessary, as the filter characteristics have already been restored. The final configuration is depicted in Fig. 1(e).

III. Design Example

A. Design and Simulation of the Filter

As said above, the first step of the procedure consists of the design of an isolated bandpass filter that, in this example, will have $N = 4$, $f_1 = 98.5$ GHz, $f_2 = 104.5$ GHz, and *RL* better than

TABLE I
DIMENSIONS OF THE FILTER AND THE FILTERING ANTENNA (MM)

Parameter	Filter	Filtering Antenna with Radiating Aperture	Filtering Antenna with Slot Array
$L_1 = L_2 = L_3 / L_4$	5.90 / 5.90	5.90 / 6	5.90 / 5.93
$W_1 = W_2 = W_3 = W_4$	2.32	2.32	2.32
t_1 / t_4	0.72 / 0.72	0.72 /-	0.72 /-
$t_{12} = t_{23} = t_{34}$	0.66	0.66	0.66
w_1 / w_4	1.62 / 1.62	1.62 /-	1.65 /-
w_{12} / w_{23}	1.75 / 1.92	1.75 / 1.92	1.75 / 1.92
w_{34}	1.75	1.73	1.78
Offset iris $k_{i,\,i+1}$ / $Q_{ext1,\,N}$	4.05 / 4.15	4.05 / 4.15	4.05 / 4.15
H_{ap} /Aperture Offset	-	1.15 / 5.95	1.65 /-
l / b	-	2 / 1.2	1.62 / 0.48
H_p	0.5	0.5	0.5
w_r / w_t / L_t	-	-	0.35 / 1.15 / 1.08
L_{r1} / L_{r2} / L_{r3}	-	-	5.22 / 0.64 / 0.25
d_{s1} / d_{s2}	-	-	1.85 / 0.68
H_{r1} / H_{r2}	-	-	0.69 / 0.31

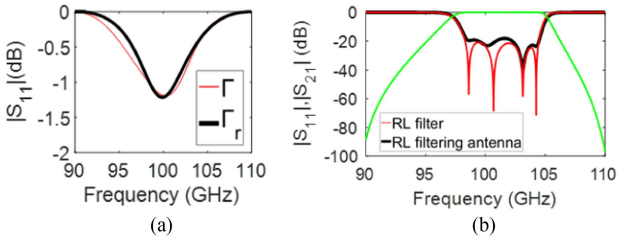

Fig. 2. Filtering antenna using a radiation aperture as a radiation element: (a) Comparison of the reflection coefficient of the FOS and ROS; (b) comparison between the return losses of the filter and of the filtering antenna.

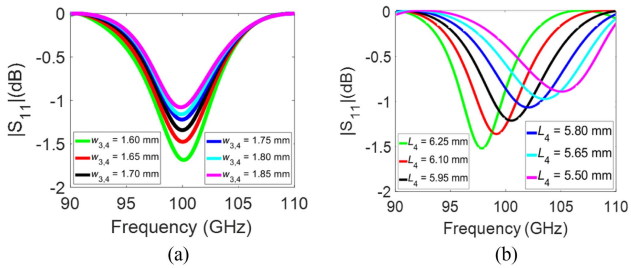

Fig. 3. Reflection coefficient (Γ_r) of the ROS achieved by modifying: (a) Iris width, $w_{3,4}$, and (b) the cavity length, L_4.

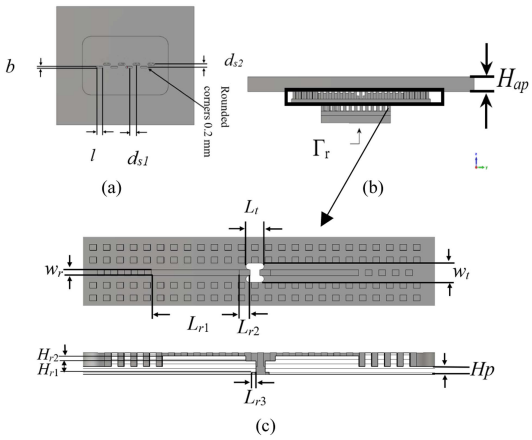

Fig. 4. Filtering antenna using a slotted RGW structure as a radiation element. (a) Top view of the radiation element; (b) schematic of the ROS; (c) top and cross-section view of the ridge waveguide layer of the ROS; and (d) schematic view of the final filtering antenna.

20 dB, using standard WR8 waveguide ports. By using (1) and (2), the following $Q_{ext1,N}$ and $k_{i,i+1}$ values can be obtained: $Q_{ext1,N} = 20.41$, $k_{12} = k_{34} = 0.054$, and $k_{23} = 0.041$. The implementation technology will be GGW, employing the zero-gap waveguide topology utilized in [18]. The GGW dimensions are as follows: $h = 0.86$ mm, $r_w = 0.35$ mm, $r_l = 0.40$ mm, and $p = 0.40$ mm [see Fig. 1(e)].

As discussed in Section II, the higher-order TE_{103} mode has been chosen to design a device more robust to manufacturing tolerances and the couplings have been implemented using an iris in the bottom wall of the cavities. A cross section of the filter can be observed in Fig. 1(a), and the corresponding dimensions are provided in Table I. The simulated filter response is shown in Fig. 2(b), where the $|S_{21}|$ is shown in the green line and the $|S_{11}|$ in the red line.

B. Design and Simulation of the Filtering Antenna With a Single Aperture as the Radiation Element

Following the matching reflection coefficient-based method explained in Section II, a filtering antenna will be implemented, integrating the previously designed BPF and a radiation element based on an aperture [19]. Once the filter has been designed, the second step involves isolating the FOS, see Fig. 1(c), to obtain its reflection coefficient, Γ, shown in Fig. 2(a). In the third step, we consider the ROS, which includes the desired radiation element, i.e., a radiation aperture in this case. The ROS, see Fig. 1(d), is evaluated to obtain its reflection coefficient, Γ_r, and the aim now is to adjust the physical parameters of the ROS to replicate the reflection coefficient of the FOS without altering the radiation characteristics. To this end, we identify in this case the length of the last resonating cavity, L_4, and the last coupling iris width, $w_{3,4}$, as the parameters that can be adjusted without modifying the radiating characteristics of the antenna used. Fig. 3 shows how Γ_r varies as the cavity length and iris width are modified. The influence of the iris width in the magnitude of the Γ_r is shown in Fig. 3(a), while Fig. 3(b) shows how to shift the frequency resonance by adjusting the cavity length. The comparison between the reflection coefficient of the FOS (red line) and the ROS (black line) after adjusting these two parameters is presented in Fig. 2(a), where a good agreement is obtained. Finally, we physically replace the FOS with the ROS to have the final component. As explained previously, when Γ_r closely matches Γ, no further optimization is necessary. Fig. 2(b) illustrates the comparison between the return loss of the BPF and the filtering antenna shown in Fig. 1(e). The dimensions of the final design are included in Table I.

C. Design and Simulation of the Filtering Antenna With a Slotted RGW Array as the Radiation Element

As shown in Fig. 4, an 8-element center-fed slot array antenna based on RGW [18] will be used in this example to explore the feasibility of the matching reflection coefficient-based method with a more complex radiation element. The radiating characteristics are primarily determined by the dimensions of the slotted aperture, such as the slot length l, slot offset d_{s2} and the longitudinal spacing d_{s1}, which can be well chosen to achieve in-phase radiation at each slot within a desired bandwidth.

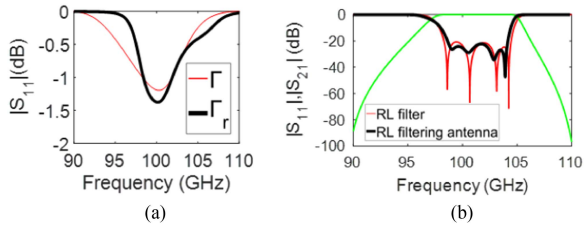

Fig. 5. Simulated *S*-parameters of the filtering antenna using a slotted RGW array as a radiation element: (a) Comparison of the reflection coefficient of the FOS and of the ROS; (b) comparison between the return losses of the filter and of the filtering antenna.

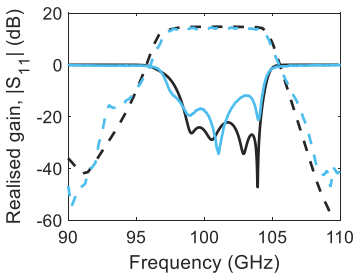

Fig. 6. Comparison between the simulated *S*-parameters of the filtering antenna (black line) and its measurements (blue line): $|S_{11}|$ in solid line and realized gain in dashed line.

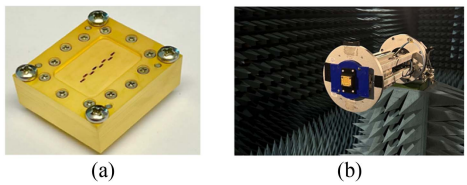

Fig. 7. Photographs of (a) fabricated prototype and (b) measurement setup.

Therefore, the length of the last resonating cavity, L_4, the last coupling iris width, $w_{3,4}$, and the parameters of the ridge and center-located coupling hole, including L_{r1}, L_{r2}, H_{r1}, H_{r2}, w_t, and L_t have been identified to adjust Γ_r without affecting the radiation characteristics. Although in this case the number of variables and, therefore, the complexity is also larger, a good similarity between the reflection coefficients of the FOS and the ROS can be observed in Fig. 5(a). In order to consider the effect of the rounded corners included in the geometry to be fabricated by CNC milling (radius equal to 0.2 mm) and compensate that the similarity between the reflection coefficients Γ and Γ_r is not as identical as in the previous example, a minor optimization is required in this case. The final dimensions are in Table I. Fig. 5(b) illustrates the comparison between the return loss of the BPF and the filtering antenna, while Fig. 6 shows the gain of the device across the passband.

IV. Manufacturing and Measurements

The second filtering antenna design has been manufactured in brass employing traditional CNC milling and, afterwards, gold plated. Photographs of the fabricated filtering antenna and the measurement setup are shown in Fig. 7. In Fig. 6, a good measured filtering performance is shown, with an average return loss level of 14 dB and a centered passband. Furthermore, the filtering antenna shows a measured gain of more than 14.5 dBi, close to the simulations along the whole passband. Fig. 8 shows the simulated and measured radiation patterns of the filtering antenna at 98.5 GHz, 101.5 GHz, and 104.5 GHz in both

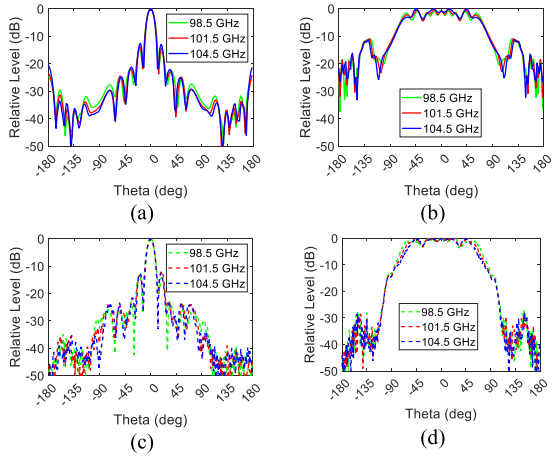

Fig. 8. Normalized radiation patterns of the filtering antenna with the slotted RGW array at 98.5 GHz, 101.5 GHz, and 104.5 GHz: (a) H-plane simulation; (b) E-plane simulation; (c) H-plane measurements; and (d) E-plane measurements.

TABLE II
Comparison of the Filtering Antenna With Other Previous Works in GGW Technology

Ref.	Frequency, f_0	BW	Max. gain	Cavity resonant mode
[10]	30.5 GHz	6.30%	8.5 dBi	TE_{101}
[11]	35.25 GHz	4.30%	26 dBi	TE_{101}
[12]	28.21 GHz	2.30%	30 dBi	TE_{101}
[13]	60 GHz	1.67%	14.7 dBi	TE_{120} & TE_{220}
[14]	14 GHz	1.20%	13.75 dBi	TE_{101}
This work	**101.5 GHz**	**6%**	**14.5 dBi**	**TE_{103}**

The bold entities correspond to the characteristics of the device proposed in this letter.

H- and E-planes. As observed, the sidelobe level is below 13 dB in the H-plane. Generally, there is a good match between the measured and simulated results, and the discrepancies can be caused by fabrication inaccuracies and the employment of a metal frame to measure the radiation pattern. A comparison with previous works on filtering antennas implemented in GGW is presented in Table II, where it can be seen that the proposed device with a slotted RGW array merits high capabilities and is very suitable for millimeter-wave frequency range applications, being the first filtering antenna operating at W-band. In contrast to the previous works referenced in the table, the use of a single higher-order mode cavity configuration ensures the required robustness against the manufacturing tolerances.

V. Conclusion

This letter introduces a matching reflection coefficient-based method for filtering antennas at W-band. To demonstrate the usefulness of the proposed technique, two different prototypes were designed in GGW technology, each one incorporating different radiation elements. The first design featured a radiation aperture, while the second prototype used a slotted RGW antenna. The second prototype was manufactured using CNC milling. The agreement between measurements and simulations highlights the usefulness of this approach and paves the way for the design of high-performance and high-frequency filtering antennas. Moreover, the method can be used in other microwave technologies, such as microstrip or SIW, also allowing the design of filtering antennas in other frequency ranges.

REFERENCES

[1] C. X. Mao, Y. Zhang, X. Y. Zhang, P. Xiao, Y. Wang, and S. Gao, "Filtering antennas: Design methods and recent developments," *IEEE Microw. Mag.*, vol. 22, no. 11, pp. 52–63, Nov. 2021.

[2] C. Chen, "A compact wideband endfire filtering antenna inspired by a uniplanar microstrip antenna," *IEEE Antennas Wireless Propag. Lett.*, vol. 21, no. 4, pp. 853–857, Apr. 2022.

[3] C. Chen, "A wideband coplanar L-probe-fed slot-loaded rectangular filtering microstrip patch antenna with high selectivity," *IEEE Antennas Wireless Propag. Lett.*, vol. 21, no. 6, pp. 1134–1138, Jun. 2022.

[4] R. Lovato and X. Gong, "A third-order SIW-integrated filter/antenna using two resonant cavities," *IEEE Antennas Wireless Propag. Lett.*, vol. 17, no. 3, pp. 505–508, Mar. 2018.

[5] P. K. Li, C. J. You, H. F. Yu, X. Li, Y. W. Yang, and J. H. Deng, "Codesigned high-efficiency single-layered substrate integrated waveguide filtering antenna with a controllable radiation null," *IEEE Antennas Wireless Propag. Lett.*, vol. 17, no. 2, pp. 295–298, Feb. 2018.

[6] R. H. Mahmud and M. J. Lancaster, "High-gain and wide-bandwidth filtering planar antenna array-based solely on resonators," *IEEE Trans. Antennas Propag.*, vol. 65, no. 5, pp. 2367–2375, May 2017.

[7] F.-C. Chen, J.-F. Chen, Q.-X. Chu, and M. J. Lancaster, "X-band waveguide filtering antenna array with nonuniform feed structure," *IEEE Trans. Microw. Theory Techn.*, vol. 65, no. 12, pp. 4843–4850, Dec. 2017.

[8] Z. Wu, J. Chen, A. Zhang, X. Lu, and X. Zhang, "Design of dual-mode dual-band rectangular waveguide filtering antenna," *Int. J. RF Microw. Comput.-Aided Eng.*, vol. 29, no. 7, 2019, Art. no. e21727.

[9] E. Rajo-Iglesias, M. Ferrando-Rocher, and A. U. Zaman, "Gap waveguide technology for millimeter-wave antenna systems," *IEEE Commun. Mag.*, vol. 56, no. 7, pp. 14–20, Jul. 2018.

[10] B. Al-Juboori, J. Zhou, and Y. Huang, "A slot filtenna based on gap waveguide using novel sidewalls," in *Proc. IEEE MTT-S Int. Microw. Filter Workshop*, 2021, pp. 162–164.

[11] Y. Shi, X. Ni, Z. Qian, S. He, and W. Feng, "Ka-band filtering antenna based on gap waveguide technology," *IEEE Antennas Wireless Propag. Lett.*, vol. 22, no. 12, pp. 3097–3101, Dec. 2023.

[12] A. Vosoogh, M. S. Sorkherizi, A. U. Zaman, J. Yang, and A. A. Kishk, "An integrated Ka-band diplexer-antenna array module based on gap waveguide technology with simple mechanical assembly and no electrical contact requirements," *IEEE Trans. Microw. Theory Techn.*, vol. 66, no. 2, pp. 962–972, Feb. 2018.

[13] C. Chen, J. Chen, P. Yan, L. Wen, and W. Hong, "Design of a 60 GHz slot filtenna array using gap waveguide feed network," *IEEE Antennas Wireless Propag. Lett.*, vol. 23, no. 2, pp. 668–672, Feb. 2024.

[14] H. S. Farahani and W. Bösch, "A novel compact high-gain filtenna using gap waveguide technology," in *Proc. IEEE Int. Symp. Antennas Propag. USNC-URSI Radio Sci. Meeting*, 2019, pp. 2043–2044.

[15] B. Ahmadi and A. Banai, "Direct coupled resonator filters realized by gap waveguide technology," *IEEE Trans. Microw. Theory Techn.*, vol. 63, no. 10, pp. 3445–3452, Oct. 2015.

[16] D. Santiago et al., "Robust design of 3D-printed W-band bandpass filters using gap waveguide technology," *J. Infrared, Millimeter Terahertz Waves*, vol. 44, no. 11, pp. 98–109, Dec. 2022.

[17] R. Cameron, C. Kudsia, and R. Mansour, *Microwave Filters for Communication Systems*. Hoboken, NJ, USA: Wiley, 2018.

[18] M. Fang, J. Yang, and A. U. Zaman, "Design of a gap waveguide based unit cell for 1-D beam scanning application at W-band," in *Proc. 17th Eur. Conf. Antennas Propag.*, 2023, pp. 1–4.

[19] J. L. Volakis, *Antenna Engineering Handbook*. New York, NY, USA: McGraw-Hill, 2007.